SCF Study of Amphiphilic Micellar Shells Containing Polyelectrolyte and Hydrophobic Sequences

Karel Jelínek, Zuzana Limpouchová, Filip Uhlík, and Karel Procházka*

Department of Physical and Macromolecular Chemistry & Laboratory of Specialty Polymers, Charles University in Prague, Faculty of Science, Albertov 6, 128 43 Praha 2, Czech Republic

Received April 20, 2007

ABSTRACT: The behavior of amphiphilic polyelectrolyte shells of micelles with kinetically frozen hydrophobic cores in aqueous solutions was studied by self-consistent field calculations. The calculations emulate the behavior of annealed (weak) shell-forming polyelectrolyte chains, e.g., poly(methacrylic acid), PMA, containing a relatively low fraction of strongly hydrophobic units, e.g., polystyrene, PS. The hydrophobic units are arranged either in sequences, or are distributed uniformly in the shell-forming chains. The analysis of concentration profiles of individual species reveals strong segregation and important self-organization of hydrophobic units in the shell. Hydrophobic units either adsorb at the core, or form small hydrophobic domains relatively far from the core. The transition from one type of conformations to the other, which depends on the position of hydrophobic sequence in the polyelectrolyte chain, can be provoked by changes in pH and ionic strength. The behavior of shell-forming chains composed of a long inner polyelectrolyte sequence (grafted to the micellar core), a short middle hydrophobic sequence and a peripheral polyelectrolyte sequence is of interest. The calculations yield a bimodal distribution of hydrophobic units as a function of the radial distance from the core/shell interface. It means that two types of chains (fairly stretched and loop-forming ones) coexist in the shell.

Introduction

The up-to-date development of pharmaceutical industry and other advanced technologies promotes the research of stimuli-responsive nanoparticles and nanostructured polymeric systems that can be used as drug carriers, nanodevices, etc. The successful exploitation of designed and developed systems requires studies of their structure-properties-function relationship. Associates of diblock copolymers (micelles and vesicles) with water-soluble shells are suitable systems for biological and pharmaceutical applications and therefore they have been studied by a number of research groups.[1−11] Recent advances in polymer synthesis resulted in the preparation of new tailored-made polymers, e.g., special copolymers and modified polyelectrolytes.[12] Polyelectrolytes represent an interesting class of practically important stimuli-responsive systems. Thanks to their properties that can be tuned by variation of external parameters and to promising potential applications, the self-assembling amphiphilic polyelectrolytes (mainly block polyelectrolytes) have been amply studied both by theoreticians[13−19] and experimentalists.[20,21] In recent years, the association of complex stimuli-responsive systems has also been studied, namely the association of triblocks,[22−28] multiblocks[29] and gradient copolymers.[30] Simultaneously the self-assembly of stars[31−34] and comb copolymers,[35] mixtures of different copolymers[36−38] leading, e.g., to onion micelles[39−41] and to the formation of interpolymer nanoparticles[42,43] have also been investigated.

We have been studying micelles with homogeneous shells formed by annealed (weak) polyelectrolytes in aqueous solutions by a combination of several experimental techniques and also by computer simulations for almost two decades. So far we studied mainly the simple core/shell systems with annealed polyelectrolyte shells. Their behavior is very rich and challenging from the theoretical point of view, e.g., under certain circumstances, we observed a nonmonotonous dependence of the gyration radius on pH.[44−47] We also found that a slight modification of the shell-forming chains by a small hydrophobic unit at the free end provokes significant changes in the pH-dependent behavior.[44,45]

At present, we continue in this direction and study the more profoundly modified polyelectrolyte systems. In this paper, we focus on kinetically frozen micelles with segmented amphiphilic shell-forming chains composed of polyelectrolyte and neutral hydrophobic sequences. Suitable copolymers are just being synthesized and results of our experimental study will be published in the future. Here we present the self-consistent field (SCF) prediction of their behavior. We would like to point out that neither the existing analytical theories, nor the molecular dynamics simulation can adequately describe the behavior of shells formed by annealed polyelectrolyte chains containing hydrophobic sequences and only SCF or Monte Carlo simulations (MC) can yield a reliable prediction. We performed both SCF and MC studies. Results of MC simulations and a systematic comparison of SCF and MC data will be published in separate papers.

Model

We study the conformational behavior of micellar shells composed of polyelectrolyte (E) and hydrophobic (H) units. We consider micelles with kinetically frozen hydrophobic cores, i.e., we assume that neither the association number nor the size of the core change in a broad range of conditions and that the shell behaves as a spherical polymer brush formed by chains with a constant length tethered to the core. Because the systems we model have not yet been studied experimentally, in the first approximation we assume that basic characteristics of micelles with 10% modified shell-forming chains (such as the association number and the size of the core) are similar to those formed by PS−PMA micelles with the same length of blocks. Hence, we use the parameters that were optimized in our earlier studies[45−47] and that reproduce the structure of the experimentally studied

* To whom correspondence should be sent. E-mail: prochaz@vivien.natur.cuni.cz.

10.1021/ma070928c CCC: $37.00
Published on Web 09/12/2007

Scheme 1. The Studied Systems: (Top) Sequenced Chain-Forming Copolymer Chains E1−H1−E2−H2−E3 and E1−H−E2 and Alternating Copolymer $[E_9H_1]_{10}$ Chain; (Bottom) Different Types of Conformations of Shell-Forming Chains[a]

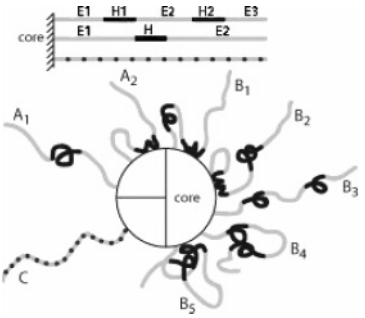

[a] These are stretched and loop-forming E1−H−E2 chains (A1 and A2, respectively), stretched (B3) and one loop-forming (B1, B2, and B4) or two loop-forming E1−H1−E2−H2−E3 chains (B5) and Alternating Copolymer $[E_9H_1]_{10}$ chains (C). The E and H units are represented by gray and black colors, respectively.

micelles, i.e., we keep the ratio of the contour length of the shell-forming chains to the radius of the compact PS core and the association number close to experimental values. Because SCF is, in principle, a parametric method, this choice should not affect general results. However, a proper selection of parameters is useful because it allows for comparison with experimental data. The pertinent values are discussed in the next part. We investigate several systems with the same length of the shell-forming block (100 monomer units), differing in the distribution of H units. Because the simple generic core/shell micelles are formed by diblock copolymers, we do not use the term "block" for shorter polyelectrolyte or hydrophobic sequences in the shell-forming block to avoid possible confusion. We speak of the shell-forming chains and E or H sequences, instead. The types of studied systems are listed below and shown in Scheme 1.

(a) First, we study segmented E1-H-E2 systems containing an inner weak polyelectrolyte sequence, E1 with a variable number of units, n_{E1}, a single neutral and hydrophobic H sequence with the following numbers of units, $n_H = 10$, 20, and 32, and a peripheral E2 sequence with n_{E2} units, The behavior of this system is discussed in detail, even though only a small part of the data was included in the paper.[48]

(b) A series of calculations was performed for segmented E1−H1−E2−H2−E3 systems containing an inner E1 sequence with n_{E1} units, the first hydrophobic H1 sequence containing $n_{H1} = 10$ or 16 units, the second (medium) E2 sequence with n_{E2} units, the second H2 sequence with the same number of units as H1, $n_{H1} = n_{H2}$, and the third (peripheral) E3 sequence containing n_{E3} units.

(c) Furthermore, we studied alternating copolymers composed of polyelectrolyte and hydrophobic units, $[E_nH_m]_k$, for $(n; m) = (9; 1)$, (8; 2) and (4; 1) and $k = (10$ or 20). The system $[E_9H_1]_{10}$ is used as a reference system for comparison with segmented systems with the same number of H units.

(d) The behavior of a homogeneous PMA shell, which we studied by several experimental methods[44,45] and by simulations,[46,47] is discussed when necessary.

Our model mimics the behavior of polymeric micelles in very dilute solutions where intermicellar interactions can be neglected and therefore we perform calculations for a single micelle only. On the basis of a number of experimental studies,[21,49] we assume that micelles formed by copolymers with comparably long core- and shell-forming blocks are on average spherical objects. Hence, we perform simulations on a spherical lattice with the origin in the center of the spherical core. Using the self-consistent-field method developed by Scheutjens and Fleer,[50] we model the micellar shell as a brush tethered to the spherical core formed by hydrophobic blocks. The shell-forming polymer chains, containing hydrophobic and both dissociated (ionized) and nondissociated (neutral) weak polyelectrolyte units, are modeled as the first-order Markov chain, which means that the position of a given unit is assumed to depend only on the position of the immediately preceding unit. The steps in all possible directions, including the reversal step, are allowed. The fundamentals of this method for annealed polyelectrolytes, as well as the computational scheme, were described in detail in a number of articles.[50−52]

All lattice sites unoccupied by copolymer units are occupied by the solvent. The solvent is an effective solvent composed of all nonpolymeric components of the system, i.e., H_2O, H_3O^+, OH^-, Na^+, and Cl^-. By setting the concentration of H_3O^+, we adjust pH and by setting the concentration of Na^+ and Cl^-, we tune the ionic strength of the solvent (expressed in mol/L).

As already mentioned, the parameters used were optimized in our earlier studies and ensure the reproduction of basic structure characteristics of similar experimentally studied systems (generic polystyrene-*block*-poly(methacrylic acid), PS−PMA micelles with the same length of blocks in aqueous media), such as the ratio of the contour length of the shell-forming blocks to the core radius. Hence we use the following parameters:[47] aggregation number, $N_{agg} = 113$, $R_c = 12$ nm (experimental values of PS−PMA micelles), effective number of the shell-forming units, $N = 100$; core radius, and the lattice constant, $l = 1$ nm (optimized coarse-grained values). For the Flory−Huggins interaction parameters, we use χ(core−solvent) = 5.0, χ(H−solvent) = 5.0, and χ(PE−solvent) = 0.5. The value for the H-solvent interaction parameter reflects the fact that water is a strong precipitant for nonpolar polymers, such as polystyrene. Auxiliary calculations showed that its variation in the range 5.0 − 10.0 does not almost influence results of SCF calculations. We use χ(H−solvent) = 5.0, because the solution of SCF equations slows down with increasing χ(H−solvent) and for $\chi = 5.0$, it still converges relatively fast. The value χ(E−solvent) = 0.5 respects the fact that water is, in the first approximation, the Θ-solvent for nonionized PMA.[53] We would like to point out that we describe short-range interactions by the Flory−Huggins parameters of individual polymer components (including the core) with the effective solvent only. It means that all homointeractions and heterointeractions (except those with solvent) equal zero, i.e., also χ(H−E) = 0.0. Hence the incompatibility of H and E units is accounted for indirectly by modeling the solvent selectivity. For the dissociation constant of PMA we use a constant literature value, $pK_A = 4.69$.[54] We use parameters for PS and PMA, because we have been studying the PS−PMA systems both experimentally and by computer simulations for a long time. At the semiquantitative level, the study describes the behavior of any sequenced annealed polyelectrolyte and hydrophobic copolymer of the above type. The application for individual systems does not require any modification, only the use of appropriate values of interaction parameters and dissociation constant.

Results and Discussion

The conformational behavior of micellar shells formed by segmented (hydrophobically modified) polyelectrolyte chains is a complex result of enthalpy-to-entropy interplay. For the discussion of the behavior, it is useful to identify the most important contributions to the enthalpy and entropy (even though

not all of them appear explicitly as independent terms in SCF equations) and to analyze their role. The enthalpy comprises several decisive contributions: (i) Hydrophobic interactions, i.e., effectively attractive short-range interactions between hydrophobic units (and also between hydrophobic units and the core) are the first. They are modeled by a combination of strongly repulsive H-solvent, weakly repulsive E-solvent and zero H-E interaction parameters. (ii) Weakly repulsive interactions between nonionized E units and solvent reflect the fact that water is at ambient temperature approximately the Θ-solvent for nonionized PMA. (iii) Long-range electrostatic interactions between dissociated polyelectrolyte groups and small ions are both attractive and repulsive (depending on the charges of species involved). For the purpose of the discussion, the entropy term can be decomposed in the following decisive contributions: conformational entropy of tethered polymer chains, entropy of mixing and translational entropy of small ions.

Behavior of Segmented E1—H—E2 Systems. At first we present selected results for segmented E1−H−E2 systems with 10% of neutral hydrophobic units ($n_H = 10$). The structure of E1−H−E2 shell depends not only on pH and ionic strength but also on the location, i.e., on "the contour position" of the H sequence, which we characterize by the E1 length, n_{E1}.

The conformational behavior at medium pH (close to pK_A) and at elevated pH is very interesting and depends strongly on the contour position of the H sequence. At low and medium ionic strengths, a nonscreened electrostatic repulsion between ionized E units (we assume a polyacid) together with the entropy-controlled behavior of counterions try to stretch the E sequences in the radial direction, while the middle H sequences partially collapse and try either to reside close to the hydrophobic core or create hydrophobic domains at longer distances from the core. The observed nontrivial conformational behavior can be explained with the help of calculated number fractions of individual units (Figure 1). The number fraction of units of a given type in a given spherical layer, $F_i(r)$ is calculated as the number of pertinent units in this layer divided by the total number of all shell-forming polymer units in this spherical layer and does not reflect the shell density. The number fractions of units are presented as functions of the distance from the core/shell interface.

The results of calculations for medium pH 5 and medium ionic strength, $I = 0.01$, can be outlined as follows: For short E1 sequences, the enthalpy-to-entropy interplay results in the formation of E1 loops (see chain A2 in Scheme 1) as it is evidenced by number fractions, $F_i(r)$ of individual monomer units. Figure 1a depicts the number fractions for $n_{E1} = 30$. The formation of loops, which allows for a close approach of H units to the nonpolar core, is favorable from the enthalpy point of view, but it lowers entropy of the shell. With increasing E1 length, we witness an interesting change in the conformational behavior (Figure 1b for $n_{E1} = 50$). The radial distribution of H units becomes bimodal. It means that some shell-forming chains still form loops, while the other are fairly stretched. The H units of partially stretched chains form a distinct spherical "hydrophobic stripe" quite far from the core, more precisely the stripe of small hydrophobic domains (see the next parts). In our earlier studies,[44,45] we observed a similar behavior of the hydrophobically end-modified shell-forming chains of PS−PMA micelles.

The distributions of E1 and E2 units in the shell are also interesting. We will focus only on the system with the bimodal distribution of H units (see Figure 1b for pH 5, ionic strength $I = 0.01$ and $n_{E1} = 50$). Because of the recoil of some E1 sequences and the "condensation" of a fraction of hydrophobic

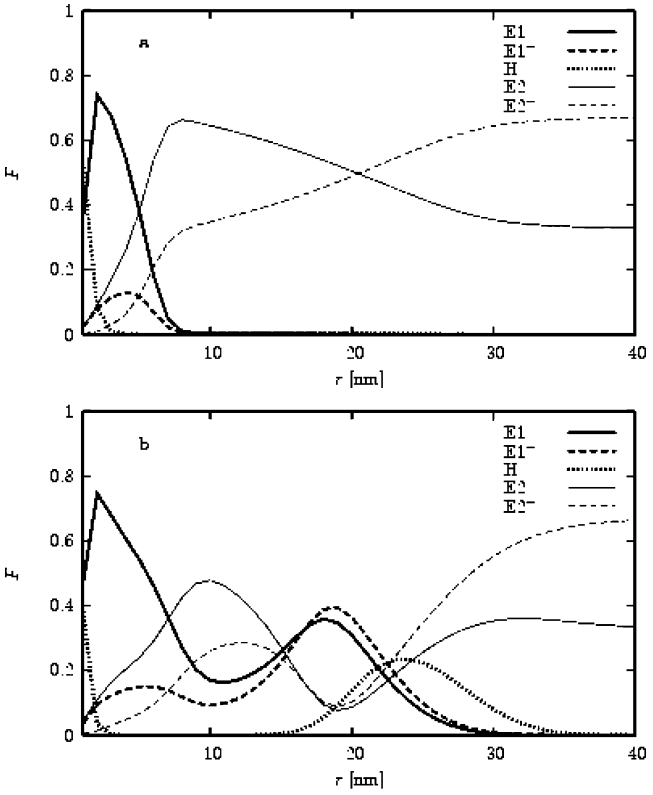

Figure 1. Number fractions, F, of H units (dotted line) and of both dissociated (dashed line) and nondisociated units (solid line) of the inner E1 (bold line) and the peripheral E2 block (thin line), respectively, as functions of the distance, r, from the core−shell interface for the system E1−H−E2, pH 5, $I = 0.01$ mol/L and (a) $n_{E1} = 30$ and (b) for $n_{E1} = 50$.

units close to the core, a nonnegligible number of peripheral E2 sequences start close to the core. Hence the number fractions of both dissociated (ionized) and nondissociated E2 units close to the core−shell interface are fairly high and increase in the radial direction. Because of the finite length of E2 sequences, $F_{E2}(r)$ pass maxima at the distance ca. 10 nm from the core and decrease later passing minima at the distance ca. 20 nm. In the region, where the second maximum in the number fraction of H units corresponding to the fraction of noncollapsed shell-forming chains (see chain A1 in Scheme 1) appears, the number fraction of E2 units grows again, because many stretched E2 sequences start here. The fraction, $F_{E1}(r)$ is also bimodal and the minimum is reached in the position, where E2 units attain the first maximum. The first maximum in $F_{E1}(r)$ reflects the accumulation of E1 units due to the recoil of E1 sequences and the second maximum reflects the stretched conformations.

Figure 2 shows the degree of dissociation, $\alpha(r)$ of all polyelectrolyte units, which increases in the radial direction, and the number fractions of all E1 and E2 (i.e., both dissociated and nondissociated) units. The formation of E1 loops together with the existence of the spherical stripe enriched by hydrophobic units far from the core results in the fact that some E2 units in recoiled chains concentrate in the region between the core and the hydrophobic stripe (in the region which is located 20−30 nm from the core) and their number fraction reaches 0.8 in the distance ca. 10 nm. These E2 units are very little dissociated.

In previous figures, we presented the number fractions of individual units, because they show very clearly the complex conformational behavior. However, the overall density decreases in the radial direction and the peripheral part of the shell (where

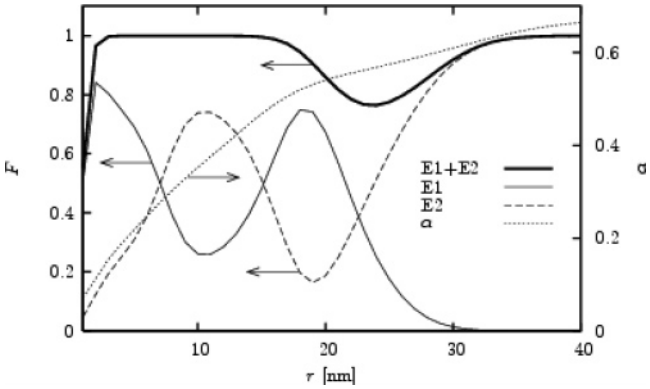

Figure 2. Number fractions, *F*, of E1 (solid line), E2 (dashed line) and of all E1 and E2 units (bold solid line) and the degree of dissociation, α, as functions of the distance, *r*, from the core−shell interface for the system E1−H−E2, pH 5, $I = 0.01$ mol/L, and $n_{E1} = 50$.

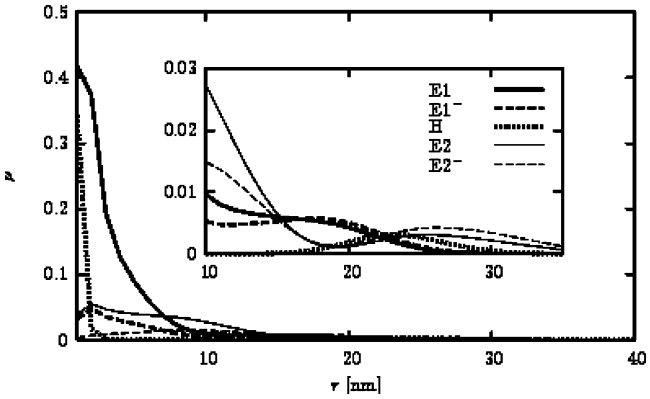

Figure 3. Volume fraction, ρ occupied by H (dotted line) and by both dissociated (dashed line) and nondisociated (solid line) units of the inner E1 (bold line) and the peripheral E2 block (thin line), respectively, as functions of the distance, *r*, from the core−shell interface for the system E1−H−E2, pH 5, $I = 0.01$ mol/L and $n_{E1} = 50$. Insert: the enlargement of volume fractions for the region of distances, $r \in \langle 10;35 \rangle$.

e.g., the second maximum in the number fraction of H units is attained) is dilute. In Figure 3, we depict the volume fractions occupied by individual components, ρ_i in spherical layers with increasing *r* (proportional to number densities). The zoom in the peripheral part (insert in Figure 3) shows clearly the nonmonotonous behavior of individual volume fractions. The experimental densities of individual units are in principle accessible by SANS for systems with selectively deuterated blocks, but due to the large difference between densities of the compact inner and the dilute peripheral parts of the shell, a fully conclusive experimental proof would be difficult.

Because the used SCF method *a priori* assumes spherical symmetry of the system and the obtained characteristics are the spherically averaged functions dependent only on the radial direction, there is a danger that the computer study is strongly influenced by this assumption and that it does not reproduce well the behavior of real micellar systems with segmented shell-forming chains. The SCF results are plausible only if the spherical symmetry is retained, i.e., if the system does not form distinct structure with lower symmetry (e.g., the Janus micelles).[55,56] To prove the symmetry assumption, we performed an independent Monte Carlo study of the same systems. The MC results will be published separately.[57] The MC study uses a model which was described in our earlier publications.[46] The simulation employs the equilibration algorithm based on the biased Rosenbluth−Rosenbluth self-avoiding walk. The short-range interactions are treated directly, while the long-range

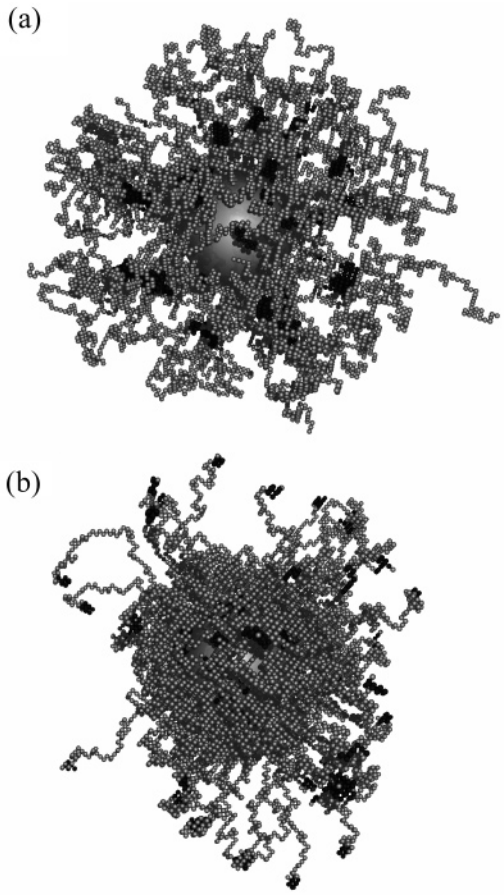

Figure 4. Snapshot of E1−H−E2 shell, pH 7, $I = 0.01$ mol/L and for $n_{E1} = 30$ (a) and $n_{E1} = 90$ (b) obtained by Monte Carlo simulations developed in refs 46 and 58 with parameters optimized in ref 47 to mimic the studied system. The gray circles represent polyelectrolyte units (both dissociated and nondissociated) and the black circles represent hydrophobic units.

electrostatic interactions are treated indirectly by solving the radial Poisson−Boltzmann (PB) equation. Both energy contributions are added and used in the Metropolis acceptance criterion, which insures the self-consistency of the used method. We assume the spherical symmetry of the electric field (which we believe is a reasonable and plausible assumption for the studied systems), but the limitations imposed by spherical symmetry have been strongly alleviated in this combined MC/PB method. Here we reproduce typical snapshots for only two E1−H−E2 systems ($n_{E1} = 30$ and $n_{E1} = 90$) at pH 7 and $I = 0.01$, Figure 4, parts a and b, respectively. The snapshots show micellar shells containing a number of small islands (domains) formed by hydrophobic units from several chains. The analysis of MC data provides the radial distribution of distances of H domains from the core and also their angular distribution and reveals that the hydrophobic domains concentrate in two spherical layers (close and far from the core), but from the angular point of view, they are randomly but quite uniformly distributed in both layers. This, we believe, (i) provides a proof that the used SCF method yields a reasonable description of the system behavior and (ii) helps to interpret the true physical meaning of the H strip as a spherical layer containing small and compact hydrophobic domains distributed on average uniformly in all directions.

An increase in pH enhances the ionization, which translates in a pronounced shell stretching. The formation of loops is less frequent at high pH and the presence of hydrophobic sequences modifies the behavior only little as compared with homogeneous

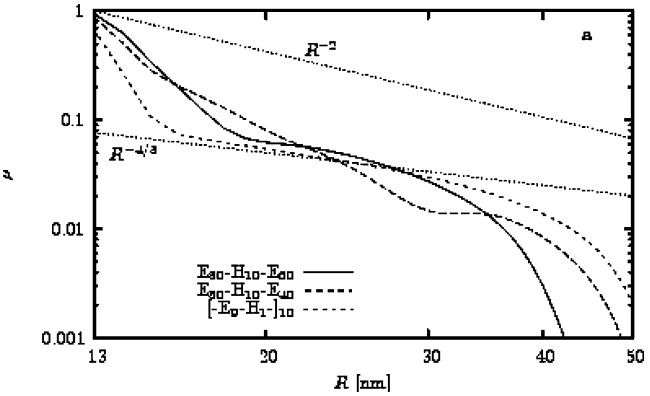

Figure 5. The log−log plot of volume fractions, ρ, of the shell-forming chains for E1-H-E2 system with $n_{E1} = 30$ (solid line), $n_{E1} = 50$ (long dashed line) and for a regular $[H_1E_9]_{10}$ system (short-dashed line) at pH 5 and $I = 0.01$ mol/L as functions of the distance R from the micellar center ($R = R_c + r$, where $R_c = 12$ nm is the core radius and r represents the distance from the core−shell interface) together with reference dependences on $R^{-4/3}$ and R^{-2} (dotted lines).

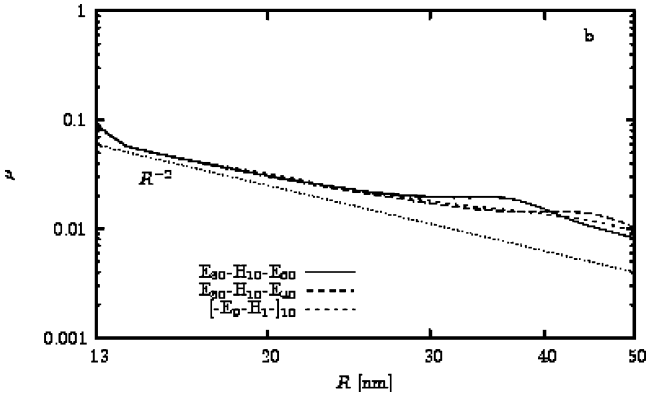

Figure 6. The log−log plot of volume fractions, ρ, of the shell-forming chains for E1−H−E2 system with $n_{E1} = 30$ (solid line) and $n_{E1} = 50$ (long dashed line) and $[H_1E_9]_{10}$ system (short-dashed line) at pH 7 and $I = 0.01$ mol/L as functions of the distance R from the micellar center ($R = R_c + r$, where $R_c = 12$ nm is the core radius and r represents the distance from the core−shell interface) together with reference dependence on R^{-2} (dotted line).

PMA shell. Nevertheless, even at high pH when the shell-forming chains are stretched, the shell is microscopically inhomogeneous and both SCF and MC indicate the presence of hydrophobic islands in both dense and dilute parts of the shell. Increasing ionic strength screens electrostatic interactions, reduces the stretching of polyelectrolyte chains, and facilitates the chain recoil and formation of loops. The electrolyte and hydrophobic units are more intermixed at higher ionic strength. The effect of pH and ionic strength on the conformational transition is discussed at the end of this section in more detail.

As already mentioned, the position of the H sequence in the chain plays important role. Figure 5 shows the log−log plots of volume fractions of monomer units in shells containing 10% of H units in one sequence ($n_{E1} = 30$ and $n_{E1} = 50$) at pH 5 and $I = 0.01$. The volume fraction occupied by polymer units is proportional to the number density (the same as in Figure 3). The log−log plot neglects the proportionality constants, which allows for a direct comparison with theoretical scaling predictions made for density profiles. We compare the curves for segmented systems with that for the alternating copolymer $[H_1E_9]_{10}$. We believe that the comparison with the alternating chain bearing the same number of hydrophobic units is more appropriate than with the PMA shell. We found that the behavior of shells formed by alternating copolymers containing low numbers of hydrophobic units is very similar to that of the pure PMA shell. For a correct discussion, it is necessary to keep in mind that the total number of all shell-forming units, which is the same for all systems, requires the multiplication by $4\pi r^2 dr$ and integration over r. For an easier discussion, we included the dash-and-dot line showing the trivial $(R_c + r)^{-2}$ dilution in the spherically symmetrical systems and the line $(R_c + r)^{-4/3}$ corresponding to the density profile of a neutral spherical brush according the Daoud and Cotton[59] scaling theory.

At relatively low pH 5 and $I = 0.01$, we see significant differences between individual systems. The inner part of the shell formed by segmented chains is crowded due to the formation of loops and the close approach of H units to the core. The volume fraction occupied by monomer units (and hence the density) is enhanced in the immediate vicinity of the core and the initial decay with r is faster than $(R_c + r)^{-2}$. It is evident that both the slope and the width of the first part depend on the position of the H sequence. This is an understandable observation because the fraction of the coreadsorbed H units decreases strongly with n_{E1}. The first region is surrounded by a layer in which the volume fraction ρ scales ca. as $(R_c + r)^{-4/3}$, which corresponds to screened electrostatics interactions.[60] The thickness of this layer decreases with n_{E1}. At the periphery, ρ drops fast as a trivial result of the finite length of chains with a broad distribution of chain stretching, however this part is only little important as it is very dilute. For comparison with the previous figures, it is necessary to keep in mind that the horizontal scale has been shifted by R_C.

At pH 7 (Figure 6), all systems are more expanded and the differences between individual systems almost disappear. Nevertheless, small differences in volume fractions at the periphery of shells are not negligible because, e.g., the contribution of individual units to the gyration radius is weighted by squares of their distances from the center. Independent of the chain architecture even at this elevated pH, a fraction of chains collapses and remains close to the core−shell interface due to strong interaction between the hydrophobic core and hydrophobic units of the shell-forming chains. The collapsed chains increase ρ close to the core and hence the initial decrease is faster than $(R_c + r)^{-2}$. In the middle part of the shell, the decrease slows down and is approximately the same for all systems. With increasing distance from the core, we observe even slower decay for segmented systems, which reflects the formation of hydrophobic domains at relatively long distances from the core. The corresponding parts of chains are more coiled and ρ decreases more slowly as compared with $(R_c + r)^{-2}$.

To conclude this part, we would like to point out that the complex structure of the shell formed by segmented chains results in log ρ − log R plots that do not strictly obey the scaling laws predicted by the theory of weak polyelectrolyte brushes,[15] but the behavior converges to that of homogeneous annealed polyelectrolyte systems with increasing pH.

The complex conformational behavior translates in interesting dependences of experimentally accessible structural characteristics, e.g., in the dependence of the gyration radius on n_{E1}. Figure 7 shows the gyration radii of E1−H−E2 shells as a function of n_{E1} for different pH and ionic strengths. It depicts the n_{E1} dependences of the net gyration radii of empty shells without micellar cores, i.e., of shells containing a cavity with a constant radius, $R_C = 12$ nm. In all cases, we see a significant increase in the gyration radius with pH and the screening effect of small ions (apparent mainly at high pH) resulting in a decrease in the size. In this respect, the behavior is similar to that of micelles with homogeneous shell-forming E blocks.

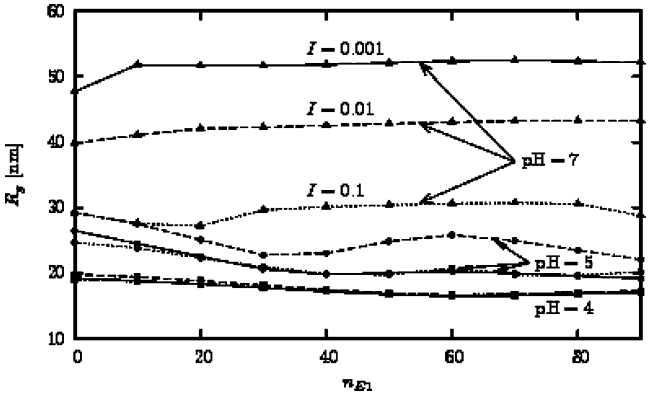

Figure 7. Gyration radius, R_g, of a copolymer shell composed of shell-forming chains containing a 10-hydrophobic-units-long H block (E1−H−E2) as a function of H block position, n_{E1}, for ionic strength I = 0.001 (solid line), 0.01 (dashed line) and 0.1 mol/L (dotted line) and several pH values.

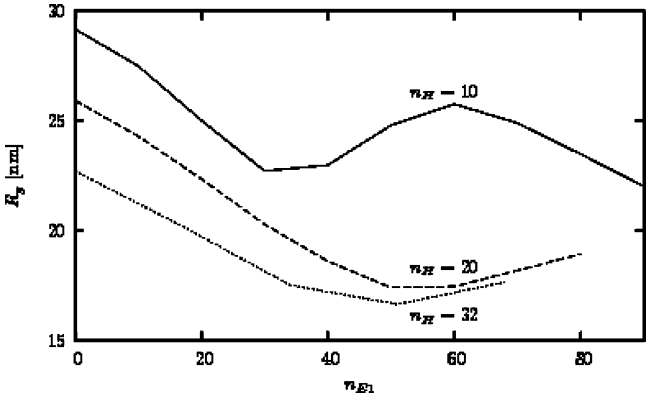

Figure 8. Gyration radius, R_g, of a copolymer shell E1-H-E2 with one hydrophobic sequence containing n_H = 10 hydrophobic units (solid line), n_H = 20 (dashed line), and n_H = 32 (dotted line) for pH 5 and ionic strength, I = 0.01 mol/L as a function of the H sequence position n_{E1}.

However, a nonmonotonous R_g dependence on the contour position of the H sequence at pH close to pK_A is an unexpected and very interesting observation. In micellar systems with relatively short E1 sequences, an increase in the E1 length results in the decrease in the gyration radius because longer E1 sequences recoil back more easily. Since the overall dissociation is low at pH close to pK_A, the E1 units are almost neutral and E1 sequences are not expanded in the vicinity of the core. The distribution of H units is bimodal in systems with intermediate E1 length and the gyration radius increases again because both E1 and E2 sequences in the nonlooping shell-forming chains are stretched in the radial direction. Finally, we observe a decrease in the gyration radius for systems with long E1 sequences. This may be explained by the fact that considerably long parts of the shell-forming chains are involved in back-looping and only relatively short E2 sequences are preferentially stretched in the radial direction. The chain ends do not reach as far from the core as in systems with shorter E1.

We studied not only the effect of the position of the H sequence on the conformations of shell-forming chains but also the effect of its length. As expected, an increase in the H length promotes the formation of E1 loops and collapse of H sequences. The shell is generally thinner and denser (its gyration radius is smaller) as compared with that of micelles with shorter H under the same conditions, but the general behavior is similar. The initial decrease in the gyration radius with increasing E1 length is more pronounced than that for systems with shorter H, but the transition from a monomodal to bimodal distribution of H units occurs approximately for the same E1 length. The comparison of gyration radii as a function of H position for systems differing in H length is shown in Figure 8.

Predictions Important for Experimental Studies. Because the aim of the study is the prediction of the behavior of micellar systems with segmented shells (which we just started to study experimentally), we would like to point out the most important findings concerning E1−H−E2 systems and their effect on the experimentally measurable properties: we have identified two decisive effects that influence the conformational behavior of shells: (i) adsorption of hydrophobic sequences at the core and (ii) formation of hydrophobic domains at longer distances from the core. We have found that under certain conditions, both structural motives coexist in the shell depending on pH, ionic strength and the position of the H sequence in the shell-forming chain.

The conformational transition provoked by external stimuli (pH and I) is particularly important, because it controls the response of the system and affects the stability and applicability of studied nanoparticles. From the experimental point of view, it is also important that the pH- and ionic-strength-dependent behavior can be studied by a combination of scattering and advanced fluorescence techniques. The SCF calculations show that changes in pH affect all studied systems. The most pronounced changes occur in systems with the H sequence in the middle of the E chain. Figure 9 compares the number fractions of H units for a system with n_{E1} = 50 at (a) pH 4, (b) pH 5, and (c) pH 7 (I = 0.01 mol/L). We see a complete conformational transition from the state with 100% adsorbed H units to the state of stretched H domains-forming chains. Similar, but less pronounced, changes are caused by ionic

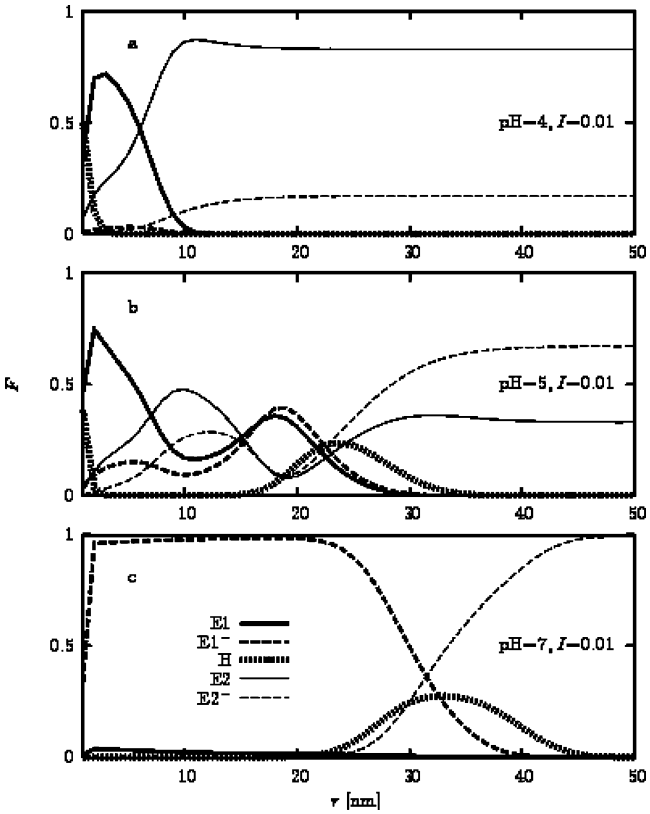

Figure 9. Number fractions, F, of H units (dotted line) and of both dissociated (dashed line) and nondisociated E units (solid line) of the inner E1 (bold line) and the peripheral E2 block (thin line), respectively, as functions of the distance, r, from the core−shell interface for a E1−H−E2 system with n_{E1} = 50 at (a) pH 4, (b) 5 and (c) 7 (I = 0.01 mol/L).

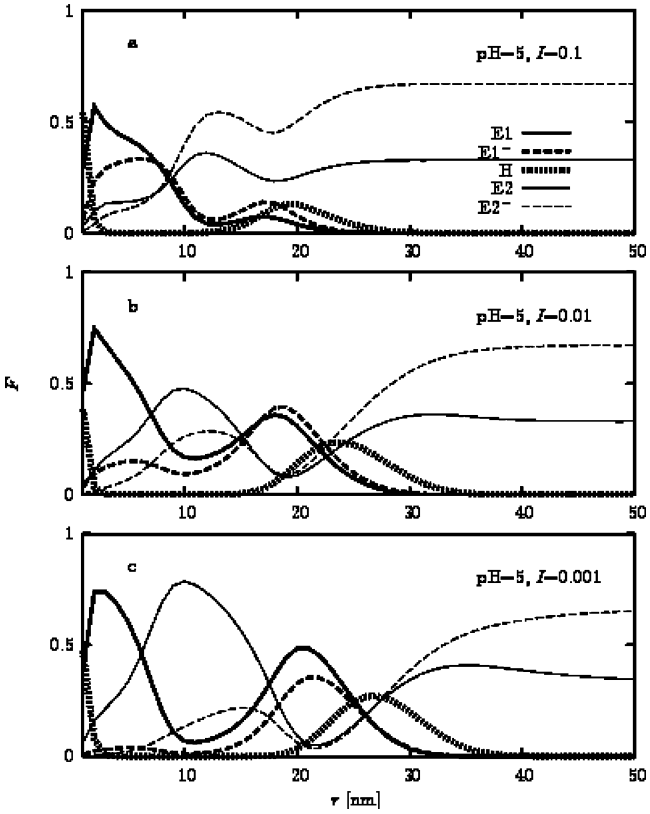

Figure 10. Number fractions, F, of H units (dotted line) and of both dissociated (dashed line) and nondisociated E units (solid line) of the inner E1 (bold line) and the peripheral E2 block (thin line), respectively, as functions of the distance, r, from the core−shell interface for a E1−H−E2 system with $n_{E1} = 50$ at (a) $I = 0.1$ mol/L, (b) 0.01, and (c) 0.001 mol/L (pH 5).

strength. Figure 10 depicts the effect of ionic strength at pH 5 for the same system. At this pH, the ionization is important and the chains are stretched. At low I, the H units form domains quite far from the core. Increasing I screens the electrostatic interactions and reduces stretching. The zone of H domains shifts closer to the core and for the highest $I = 1$, we observe a transition in the conformational behavior: a low fraction of H units adsorb at the core. Both dependences show that the transition is gradual and smooth and occurs in a broad range of conditions and that both types of chains, i.e., the loop-forming and the stretched ones coexist in a certain range of conditions.

Behavior of Shells Formed by Chains Containing More E and H Sequences. The behavior of systems with more sequences is complex. Nevertheless, such systems are practically important, because some synthetic procedures can easy produce chains containing many short sequences, e.g., the free radical polymerization of two monomers with a proper combination of rate constants of four reactions involved (i.e., with suitable copolymerization parameters). We performed an extensive study because one can imagine a broad variety of architectures of shell forming chains. In the next part, we present one example of the conformational behavior of the E1−H1−E2−H2−E3 system only. The most interesting results were obtained for systems with long E1 and E2 in solutions with a low ionic strength ($I = 0.01$) at pH 5, i.e., close to pKA. Since both E1 and E2 sequences are long and flexible, they are capable of back-looping. A careful analysis of r dependences of number fractions of units of different types for a system with $n_{H1} = n_{H2} = 10$, $n_{E1} = n_{E2} = 30$ and $n_{E3} = 20$ suggests that several types of loops form in the shell (see chains B in Scheme 1): E1 loops toward the core (chain B2) and E2 loops either to the core

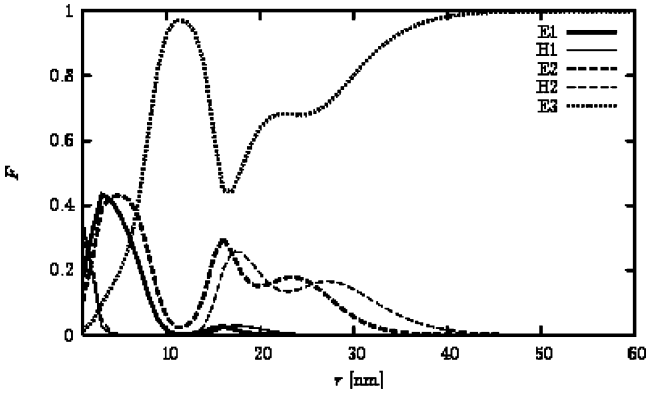

Figure 11. Number fractions, F, of all dissociated and nondissociated E1 (bold solid line), H1 (thin solid line), E2 (bold dashed line), H2 (thin dashed line), and E3 units (bold dotted line) as functions of the distance, r, from the core−shell interface for a system E1−H1−E2−H2−E3 with $n_{H1} = n_{H2} = 10$, $n_{E1} = n_{E2} = 30$, $n_{E3} = 20$, pH 5, $I = 0.1$ mol/L.

(chains B1 and B5) or to the region of the hydrophobic stripe (chain B4). The loop-formation is well documented by number fractions of hydrophobic and polyelectrolyte units as functions of the distance from the core−shell interface (Figure 11). Both curves for H1 (thin solid line) and H2 (thin dashed line) are high in a fairly narrow layer close to the core and drop very fast to zero, which is attained between 5 and 12 nm. Later they rise again and reach the first local maximum at distances between 17 to 18 nm, which indicates the formation of a well-defined spherical stripe containing increased numbers of both H1 and H2 units. The curve for H2 continues through a shallow minimum at ca. 23 nm and reaches the second flat local maximum at ca. 28 nm due to the formation of a rather broad stripe quite far from the core by the stretched chains (chain B3 in Scheme 1). It is necessary to keep in mind that the total volume fraction, ρ is very low at distances approaching 30 nm (not shown) and hydrophobic units intermix with both polyelectrolyte E2 and E3 units. As concerns the polyelectrolyte fractions, we find units of all three polyelectrolyte sequences (bold lines) quite close to the core, i.e., in the region 5−15 nm, which is consistent with the idea that a nonnegligible fraction of all E1, E2 and E3 sequences recoils back toward the core. In this graph, we do not differentiate between ionized and neutral E units in order to get a clear and comprehensive picture.

Because of the fact, that long chains can easy recoil back, a fairly high fraction of H2 units return back, very close, to the core. It is documented not only by their high fraction at small distances, but also by the fact, that E3 units (only 20 per chain) almost replace both E1 and E2 units at distances around 10 nm. When discussing this figure, one has to be careful. It is necessary to keep in mind that in contrast to volume fractions or densities, which are very low at distances longer than 20 nm, the fraction of E3 units at the periphery is one by definition because other units cannot reach so far from the core. The volume fractions were discussed in detail for E1−H−E2 systems. Since the general trend is similar, we do not show calculated curves to save the space. They decrease steeply in the radial direction and both hydrophobic stripes are very dilute. The decrease is more pronounced for E1−H1−E2−H2−E3 than for E1−H−E2 because the former system contains two times more H units and is more compact than the latter one (the fraction of back-coiled chains is higher). The total volume fraction, $\rho(r)$ is higher close to the core in the former system and decreases steeply with the distance. Nevertheless, the analysis of number fractions, $F_i(r)$ in both E1−H−E2 and E1−

H1−E2−H2−E3 systems, including the dilute peripheral parts of the shell, is very instructive. (i) It shows the behavior of individual chains (it is actually the only reasonable and illustrative way how to track the average conformational behavior of chains of different types in different parts of the shell in SCF calculations), and (ii) it reveals the strong segregation and self-organization of tethered amphiphilic chains in dilute peripheral parts of the shell (which has been proven also by MC simulations).

Conclusions

The conformations of micellar shells formed by heterogeneous chains (copolymer containing annealed polyelectrolyte and a low fraction of hydrophobic units) in aqueous solutions depend not only on pH and ionic strength but also on the fraction of hydrophobic units and their distribution. The arrangement of hydrophobic units in short sequences results in a microheterogeneous structure of the shell. We have identified two types of conformations: (i) back-looping conformations allowing the adsorption of hydrophobic units at the core and (ii) stretched conformations enabling the formation of hydrophobic domains quite far from the core. The transition from one to the other conformational type depends on the position of the hydrophobic sequence in the polyelectrolyte chain, but it can also be affected by pH and ionic strength. The transition is gradual, i.e., the entropy-to-enthalpy interplay results in a bimodal distribution of hydrophobic units which shifts in favor of the coreadsorbed ones with decreasing pH and increasing *I*.

We found that the changes in the shell structure and expansion which are the key factors ensuring the solubility and stability of micellar solutions, as well as the experimentally accessible size characteristics of micelles (like the radius of gyration) are very sensitive to the distribution of hydrophobic units. Therefore, one has to be careful, when conclusions on the stability and behavior of micellar solution are based on the average molecular characteristics only.

The most important methodological conclusion that can be drawn from the performed study is following: The application of the spherically symmetrical SCF method for studying the (on average) spherically symmetrical polymeric micelles with microheterogeneous shells are useful, but the interpretation of results is a delicate task and it has to be done with a great care and precaution. The SCF methodology captures the most important features and yields plausible information on the system behavior. A careful analysis of the data reveals the strong tendency of back-looping and the fact that a fraction of segmented chains recoil back, while the other stretch in the radial direction, which results in a bimodal distribution of chain conformations in studied systems. However, the SCF approach concentrating on the angularly averaged behavior is too coarse and does not allow for an unambiguous detailed analysis of the data. Independent information is needed for a reliable interpretation of SCF results.

On the other hand it is worth-mentioning that an additional piece of information on the qualitative level only, i.e., information on the formation of hydrophobic domains that are spherically uniformly distributed in two distinct layers (one close to and the other far from the core) provided by MC simulation justifies the assumption of the average spherical symmetry and provides sufficient hint for correct interpretation of bimodal distributions and the nature of angularly averaged hydrophobic trips. Detailed analysis of number fractions of individual parts of chains yields valuable information. Because the SCF calculations are much faster than MC, the study of a series of micellar shells differing in composition in a broad range of conditions is possible by SCF, but the same MC study would be too time-consuming.

Acknowledgment. We would like to acknowledge the financial support of the Grant Agency of the Czech Republic (Grants No. 203/07/0659 and 203/04/P117), the Grant Agency of the Academy of Sciences of the Czech Republic (Grant No. IAA401110702) and the Ministry of Education of the Czech Republic (Long-term research plan MSM0021620857. Authors thank also for the support by the Marie Curie Research and Training Network (Grant No. 505 027, POLYAMPHI). We would like to thank the Laboratory of Physical Chemistry and Colloid Science at Wageningen University, The Netherlands, namely, Dr. F. A. M. Leermarkers and Prof. G. J. Fleer, for providing the software for SCF calculations.

References and Notes

(1) Savic, R.; Eisenberg, A.; Maysinger, D. *J. Drug Target.* **2006**, *14*, 343.
(2) Azzam, T.; Eisenberg, A. *Angew. Chem., Int. Ed.* **2006**, *45*, 7443.
(3) Biggs, S.; Sakai, K.; Addison, T.; Schmid, A.; Armes, S. P.; Vamvakaki, M.; Butun, B.; Webber, G. *Adv. Mater.* **2007**, *19*, 247.
(4) Wang, D.; Yin, J.; Zhu, Z. Y.; Ge, Z. S.; Liu, H. W.; Armes, S. P.; Liu, S. Y. *Macromolecules* **2006**, *39*, 7378.
(5) Butun, V.; Liu, S.; Weaver, J. V. M.; Bories-Azeau, X.; Cai, Y.; Armes, S. P. *React. Funct. Polym.* **2006**, *66*, 157.
(6) Förster, S.; Abetz, V.; Müller, A. H. E. *Adv. Polym. Sci.* **2004**, *166*, 173.
(7) Pergushov, D. V.; Remizova, E. V.; Felthusen, J.; Zezin, A. B.; Müller, A. H. E.; Kabanov, V. A. *J. Phys. Chem. B* **2003**, *107*, 8093.
(8) O'Reilly, R. K.; Hawker, C. J.; Wooley, K. L. *Chem. Soc. Rev.* **2006**, *35*, 1068.
(9) Harada, A.; Kataoka, K. *Prog. Polym. Sci.* **2006**, *31*, 949.
(10) Mitsukami, Y.; Hashidzume, A.; Yusa, S.; Morishima, Y.; Lowe, A. B.; McCormick, C. L. *Polymer* **2006**, *47*, 4333.
(11) Förster, S.; Hermsdorf, N.; Bottcher, C.; Lindner, P. *Macromolecules* **2002**, *35*, 4096.
(12) Bohrisch, J.; Eisenbach, C. D.; Jeager, W.; Mori, H.; Müller, A. H. E.; Rehahn, M.; Schaller, C.; Traser, S.; Wittmeyer, P. *Adv. Polym. Sci.* **2004**, *165*, 1.
(13) Birshtein, T. M.; Zhulina, E. B. *Polymer* **1989**, *30*, 170−177.
(14) Wijmans, C. M.; Zhulina, E. B. *Macromolecules* **1993**, *26*, 7214−7224.
(15) Zhulina, E. B.; Birshtein, T. M.; Borisov, O. V. *Macromolecules* **1995**, *28*, 1491−1499.
(16) Shusharina, N. P.; Linse, P.; Khokhlov, A. R. *Macromolecules* **2000**, *33*, 3892−3901.
(17) Borisov, O. V.; Daoud, M. *Macromolecules* **2001**, *34*, 8286−8293.
(18) Borisov, O. V.; Zhulina, E. B. *Macromolecules* **2003**, *36*, 10029−10036.
(19) Shusharina, N. P.; Zhulina, E. B.; Dobrynin, A. V.; Rubinstein, M. *Macromolecules* **2005**, *38*, 8870−8881.
(20) Kotz, J.; Kosmella, S.; Beitz, T. *Prog. Polym. Sci.* **2001**, *26*, 1199−1232.
(21) *Hamley, I. W.: Physics of Block Copolymers*; Oxford University Press, Oxford, U.K., 1998, and references therein.
(22) Cai, Y. L.; Armes, S. P. *Macromolecules* **2004**, *37*, 7116−7122.
(23) Weaver, J. V. M.; Armes, S. P.; Liu, S. Y. *Macromolecules* **2003**, *36*, 9994−9998.
(24) Koutalas, G.; Pispas, S.; Hadjichristidis, N. *Eur. Phys. J. E* **2004**, *15*, 457−464.
(25) Li, Z. B.; Chen, Z. Y.; Cui, H. G.; Hales, K.; Qi, K.; Wooley, K. L.; Pochan, D. J. *Langmuir* **2005**, *21*, 7533−7539.
(26) Katsampas, I.; Tsitsilianis, C. *Macromolecules* **2005**, *38*, 1307−1314.
(27) Sfika, V.; Tsitsilianis, C.; Kiriy, A.; Gorodyska, G.; Stamm, M. *Macromolecules* **2004**, *37*, 9551−9560.
(28) Riegel, I. C.; Samios, D.; Petzhold, C. L.; Eisenberg, A. *Polymer* **2003**, *44*, 2117−2128.
(29) Determan, M. D.; Guo, L.; Thiyagarajan, P.; Mallapragada, S. K. *Langmuir* **2006**, *22*, 1469−1473.
(30) Karaky, K.; Pere, E.; Pouchan, C.; Garay, H.; Khoukh, A.; Francois, J.; Desbrieres, J.; Billon, L. *New J. Chem.* **2006**, *30*, 698−705.
(31) Štěpánek, M.; Matějíček, P.; Humpolíčková, J.; Havránková, J.; Podhájecká, K.; Špírková, M.; Tuzar, Z.; Tsitsilianis, C.; Procházka, K. *Polymer* **2005**, *46*, 10493−10505.
(32) Voulgaris, D.; Tsitsilianis, C.; Esselink, F. J.; Hadziioannou, G. *Polymer* **1998**, *39*, 6429−6439.

(33) Li, Z. B.; Hillmyer, M. A.; Lodge, T. B. *Langmuir* **2006**, *22*, 9409.
(34) Havránková, J.; Limpouchová, Z.; Procházka, K. *Macromol. Theory Simul.* **2005**, *14*, 560−568.
(35) Tsolakis, P.; Bokias, G. *Macromolecules* **2006**, *39*, 393−398.
(36) Matecaron;jíček, P.; Humpolíčková, J.; Procházka, K.; Tuzar, Z.; Špírková, M.; Hof, M.; Webber, S. E. *J. Phys. Chem. B* **2003**, *107*, 8232−8240.
(37) Podhájecká, K.; Štěpánek, M.; Procházka, K.; Brown, W. *Langmuir* **2001**, *17*, 4245−4250.
(38) Liu, X. Y.; Wu, Y.; Kim, J. S.; Eisenberg, A. *Langmuir* **2006**, *22*, 419.
(39) Procházka, K.; Martin, T. J.; Webber, S. E.; Munk, P. *Macromolecules* **1996**, *29*, 6526−6530.
(40) Pleštil, J.; Kříž, J.; Tuzar, Z.; Procházka, K.; Melnichenko, Yu. B.; Wignall, G. D.; Talingting, M. R.; Munk, P.; Webber, S. E. *Macromol. Chem. Phys.* **2001**, *202*, 553−563.
(41) Talingting, M. R.; Munk, P.; Webber, S. W.; Tuzar, Z. *Macromolecules* **1999**, *32*, 1593−1601.
(42) Pergushov, D. V.; Remizova, E. V.; Gradzielski, M.; Lindner, P.; Feldhusen, J.; Zezin, A. B.; Müller, A. H. E.; Kabanov, V. A. *Polymer* **2004**, *45*, 367.
(43) Cheluskhin, P. S.; Lysenko, E. A.; Bronich, T. A.; Eisenberg, A.; Kabanov, A. V.; Kabanov, V. A. *Polym. Sci. Ser. A* **2004**, *46*, 485.
(44) Matějíček, P.; Podhájecká, K.; Humpolíčková, J.; Uhlík, F.; Jelínek, K.; Limpouchová, Z.; Procházka, K.; Špírková, M. *Macromolecules* **2004**, *37*, 10141−10154.
(45) Matějíček, P.; Uhlík, F.; Limpouchová, Z.; Procházka, K.; Tuzar, Z.; Webber, S. E. *Macromolecules* **2002**, *35*, 9487−9496.
(46) Uhlík, F.; Limpouchová, Z.; Jelínek, K.; Procházka, K. *J. Chem. Phys.* **2004**, *121*, 2367−2375.
(47) Jelínek, K.; Uhlík, F.; Limpouchová, Z.; Matějíček, P.; Procházka, K. *Collect. Czech. Chem. Commun.* **2006**, *71*, 756−768.
(48) Additional data are available upon request.
(49) Tuzar, Z. In *Solvents and Self-Organization of Polymers*; Webber, S. E., Munk, P., Tuzar, Z., Eds.; Kluwer Academic Publishers: Dordrecht, The Netherlands, 1996; Vol. 327.
(50) Fleer, G. J.; Cohen Stuart, M. A.; Scheutjens, J. M. H. M.; Cosgrove, T.; Vincent, B. *Polymers at Interfaces*; Chapman & Hall: London and New York, 1993.
(51) Böhmer, M. R.; Evers, O. A.; Scheutjens, J. M. H. M. *Macromolecules* **1990**, *23*, 2288−2301.
(52) Israëls, R.; Leermakers, F. A. M.; Fleer, G. J. *Macromolecules* **1994**, *27*, 3087−3093.
(53) Kanevskaya, Ye. A.; Zubov, P. I.; Ivanova, L. V.; Lipatov, Ya. S. *Vysokomol. Soedin.* **1964**, *6*, 981; *Polym. Sci. USSR* **1964**, *6*, 1080.
(54) Lide, D. R. *CRC Handbook of Chemistry and Physics*, 76th ed.; CRC: Boca Raton, FL, 1995.
(55) Mori, H.; Muller, A. H. E. *Prog. Polym. Sci.* **2003**, *28*, 1403−1439.
(56) Erhardt, R.; Zhang, M. F.; Boker, A.; Zettl, H.; Abetz, C.; Frederik, P.; Krausch, G.; Abetz, V.; Muller, A. H. E. *J. Am. Chem. Soc.* **2003**, *125*, 3260−3267.
(57) Uhlík, F.; Limpouchová, Z.; Jelínek, K.; Procházka, K.: A Monte Carlo study of micellar shells formed by block, submitted to *Macromolecules.*
(58) Uhlík, F.; Limpouchová, Z.; Jelínek, K.; Procházka, K. *J. Chem. Phys.* **2003**, *118*, 11258−11264.
(59) Daoud, M.; Cotton, J. P. *J. Phys. (Paris)* **1982**, *43*, 531−538.
(60) Borisov, O. V.; Zhulina, E. B. *Eur. Phys. J. B* **1998**, *4*, 205−217.

MA070928C